J Mater Sci (2011) 46:659–669
DOI 10.1007/s10853-010-4788-6

# Comparison of rheological and electrical percolation phenomena in carbon black and carbon nanotube filled epoxy polymers

**Jan Sumfleth · Samuel T. Buschhorn · Karl Schulte**

Received: 23 April 2010 / Accepted: 22 July 2010 / Published online: 4 August 2010


**Abstract** Epoxy nanocomposite suspensions including multi-wall carbon nanotubes (MWCNTs) and carbon black (CB) were produced and investigated by means of combined rheological and electrical analysis. The rheological percolation behaviour was compared to the electrical percolation behaviour. Due to similar dynamic agglomeration mechanisms the difference between the rheological and the electrical percolation threshold in the cured state is identical for MWCNT and CB filled systems. Non-covalent matrix–nanoparticle interactions in uncured epoxy suspensions are negligible since the onset of electrical and rheological percolation in the uncured state coincidence. Furthermore, the electrical percolation threshold in the cured state is always lower than in the uncured state because of the high tendency of CB and MWCNTs to form conductive networks during curing. The difference between rheological and electrical percolation threshold is dependent on the curing conditions. Thus, the rheological percolation threshold can be considered as an upper limit for the electrical percolation threshold in the cured state. Due to the formation of co-supporting networks multi-filler (MWCNTs and CB) suspensions exhibit a similar rheological behaviour as the binary MWCNT suspensions. For both types of suspensions a rheological percolation threshold of around 0.2 and 0.25 wt% was determined. Conversely, the binary CB nanocomposites exhibit a four-times higher percolation threshold of about 0.8 wt%. The difference between the binary MWCNT suspension and the ternary CB/MWCNT suspension in storage shear modulus at high filler concentrations (~0.8 wt%) turns out to be less than expected. Thus, synergistic effects in network formation are already present in the epoxy suspension and get more pronounced during curing.

J. Sumfleth (✉) · S. T. Buschhorn · K. Schulte
Technische Universität Hamburg-Harburg, Institute of Polymers and Composites, Denickestr. 15, 21073 Hamburg, Germany
e-mail: jan.sumfleth@tuhh.de
URL: www.tuhh.de/kvweb

## Introduction

Since decades carbon-based particles are commonly used to impart an electrical conductivity into isolating polymers systems. Here, nano-scaled particles showed the best performance in terms of high electrical conductivities and low percolation thresholds (critical filler concentration for insulator/conductor transition) [1–3]. Nano-scaled carbon black (CB) can be considered as a good choice to obtain rather low percolation thresholds and relatively high electrical conductivities [4–7]. Nevertheless, since carbon nanotubes (CNTs) has emerged in the field of polymer science, the interest of research and technology in theses types of nanoparticles has been steadily grown due to their outstanding physical properties [8–12]. Their transfer seems to be still a great challenge since the nanocomposite properties often do not meet the theoretical predictions. However, the high aspect ratio and low intrinsic electrical resistance of CNTs lead to very high electrical conductivities and low percolation thresholds of nanocomposites filled with CNTs, especially if compared to nanocomposites filled with spherical CB [13, 14]. Lowest reported percolation thresholds are 0.0025 wt% for multi-wall carbon nanotubes (MWCNTs) [15] and 0.005 wt% for single-wall CNTs [16]. Contrarily, most of the reported percolation thresholds for various polymer systems filled with CNTs were found to be around 0.1 wt% [17 and references therein]. These low percolation thresholds

can only be explained by the presence of kinetic percolation mechanisms occurring during curing of such low viscosity epoxies. At this stage, the fine dispersed CNT distribution undergoes re-agglomeration and flocculation processes where fractal network structures are formed [18]. The tendency for such particle network re-organisations is even more pronounced in thermosets than in thermoplastics due to the low viscosity of the thermoset components before polymerisation. Nevertheless, re-agglomeration in thermoplastic melts has been observed and was subsequently studied and theoretically modelled for a variety of thermoplastic systems [19–23].

Due to the formed nanoparticle networks, the rheological properties (e.g. viscosity) of uncured epoxy suspensions are significantly increased by orders of magnitude [24, 25]. This increase in rheological properties is often referred to a 'rheological percolation' transition which has been studied for various types of carbon nanoparticle (CNTs, CB and others) suspensions based on low viscous solvents such as epoxy [24, 25], water [26–30] and other organic liquids [31, 32]. In comparison to the electrical percolation threshold, values for the rheological percolation thresholds were found at subsequently higher filler contents between 0.1 and 2 wt%, depending on the nanoparticle dispersion method and the chemical origin of the solvent. For thermoplastic systems, both percolation phenomena (electrical and rheological) have been systematically compared for a variety of thermoplastic polymers [33–39]. Depending on the type of thermoplastic polymer and the CNT dispersion method, the rheological percolation threshold is usually at lower CNT contents compared to the electrical percolation threshold [37–40]. Reasons for the different percolation thresholds for conductivity and rheology can be found in different morphological requirements for a mechanical rigid or an electrically conductive network [37–39].

Interestingly, this systematic comparison of both percolation phenomena has not been performed for thermoset polymers although extensive rheological and electrical studies were conduced [15, 16, 18, 24, 25, 41–44]. Nevertheless, some latest works by Allaoui and El Bounia [45] as well as by Chapartegui et al. [46] linked the electrical and rheological percolation features of epoxy nanocomposites and their suspensions. Chapartegui et al. [46] showed that the electrical percolation threshold (0.04 wt%) of the uncured suspensions is lower than their rheological percolation threshold (0.067–0.13 wt%) due to the absence of a combined polymer–CNT network in the low viscous epoxy pre-polymer. Contrarily, Allaoui and El Bounia [45] stated that the electrical and rheological percolation thresholds of their uncured suspensions coincidence at the same filler content of around 0.5 wt%. Both works used the same epoxy resin as well as the same type of CNTs. Thus, differences in the occurrence of rheological and electrical percolation can be directly related to different dispersion methods.

As mentioned earlier, for thermoplastic systems, the rheological and electrical percolation was described for a set of different polymers. More detailed studies about percolation in CNTs in thermoplastic systems were put forward by Alig et al. [20, 21, 40, 47], where the classical percolation theory was extended by theories based on cluster aggregation mechanisms. Latest works performed by Skipa et al. [22] and Richter et al. [23] further extended these approaches.

It has to be mentioned that a detailed description of the rheological and electrical percolation including theoretical assumptions made by the classical percolation theory are missing for epoxy systems [45, 46]. This detailed description will be given in this paper for a similar epoxy system as used by [45, 46]. Additionally, both electrical and rheological percolation thresholds of the nanoparticle (CNT and CB) filled suspensions will be systematically compared to their respective electrical percolation thresholds in the cured state which were already presented in an earlier work by the authors of the present paper [14]. In this earlier work, the electrical percolation phenomenon and their underlying mechanisms of particle network formation in CB and CNT filled epoxy nanocomposites were compared to a new class of multi-filler nanocomposites including both CB and CNTs. These multi-filler systems, containing CB and CNTs at a relative ratio of 50:50%, exhibit almost identical electrical properties as the nanocomposites only filled with CNTs revealing synergistic effects in the formation of co-supporting network of both types of nanoparticles. Other works using different combinations of conductive carbon nanoparticles found similar synergistic effects in multi-filler network formation and thus electrical conductivities of the hybrid nanocomposites [48–51]. Therefore, this paper aims two major goals: first, to compare and describe the rheological and electrical percolation transitions in CB and CNT filled epoxy systems. Second, to compare the rheological percolation transitions among the various nanocomposites systems (CNT, CB and CB/CNT). The latter approach is going to give new insights in the synergistic effects in network formation of multi-particle systems as proposed in [14].

## Experimental

The epoxy polymer is a three component system consisting of a DGEBA-based resin (LY556), an anhydride curing agent (CH917) and an amine-based accelerator (DY070), provided by Huntsman, Switzerland. The resin system exhibit good mechanical, thermal and chemical properties and is certificated for aeronautic applications. The Printex

XE2® is a spherical CB particle with a primary particle size of 30 nm, provided by Degussa-Evonik, Germany. The Graphistrength C100® are MWCNTs, exhibiting an outer diameter of about 15 nm with length of up to 10 μm, and were provided by Arkema, France. The nanoparticle filled epoxy polymers were produced using a lab-scale three-roll-mill (Exakt 120E®) which enables the introduction of very high shear forces (up to 200,000 $s^{-1}$) throughout the suspension. The nanocomposite production started with a manual distribution of the nanoparticles in the LY556 resin component. The pre-dispersed suspension was then given batchwise onto the rolls with dwell times of 2 min. The dispersive forces on the suspension were acting in the gap (5 μm) between the rolls. Details about the dispersion technique can be found in earlier publications [52, 53]. After dispersion of the nanoparticles in the resin component LY556, the hardener and accelerator are usually added in a vacuum dissolver in order to avoid trapped air in the suspension as described in [54].

In this work, a small portion of the LY556/CH917 mixture was taken before adding the accelerator in order to avoid curing of the suspensions during rheological analysis. Since the amount of the accelerator is very low (1:191 parts), the rheological response of the suspension without accelerator does not vary. The filler contents were changed in small steps from very low (0.03 wt%) to high (up to 1.6 wt%). In the multi-filler (ternary) systems, the relative ratio between CB and MWCNT was set to 50:50%, e.g., 0.2 wt% CB plus 0.2 wt% MWCNT.

Already done in our previous work, the suspensions including the accelerator were poured into aluminium moulds (100 × 180 $mm^2$) and cured in an oven for 4 h at 80 °C plus 8 h at 140 °C. After curing, samples for electrical analysis were machined out of the plates. Details about the electrical conductivity measurements and the electron microscopy analysis of the cured samples can be found in our previous work [14]. In the present work, the electrical conductivity data of the cured samples were reused for comparison of both electrical and rheological percolation.

The rheological analysis of the nanoparticle filled suspensions was performed in a TA ARES® strain-controlled rheometer with a plate–plate configuration ($d = 40$ mm). The test program included frequency sweep tests from 0.1 to 15 Hz at 25 °C at a fixed strain of 10%, ensuring the samples to be tested in the linear visco-elastic regime. As a new approach for the investigation of nanoparticle suspensions, an on-line monitoring of the electrical conductivity of the suspensions during rheological testing was performed similar to the approaches performed for thermoplastic systems by [19, 40]. The plates of the rheomoeter were electrically isolated from the device frame by PVC inlets. Additionally, the plates were wired and lead out of the rheometer by sliding contacts. Therefore, the whole plates act as electrodes. The electrical conductivity was measured with a Hewlett-Packard impedance analyser (HP 4284A LCR) at a fixed frequency of 100 Hz, which can be regarded as the DC conductivity. The conductivity data were taken directly at the start of the frequency sweep tests.

## Electron microscopy

In order to give an insight in the state of nanoparticle dispersion in the cured state, transmission electron microscopy (TEM) on the single-filler (binary) and the multi-filler (ternary) nanocomposites was conducted. Regarding the binary MWCNT system, most of the MWCNTs are individually dispersed. MWCNTs tend to form networks throughout the epoxy matrix during curing [18, 55]. These networks can be made visible in TEM, as observed in Fig. 1a. The dispersion with the three-roll-mill provides a good degree of dispersion of MWCNTs, although some primary agglomerates can still be observed (see Fig. 1a bottom). As it can be concluded from their dense structure and entanglements, such agglomerates originate from the chemical vapour deposition (CVD) production process and have not been formed by kinetic re-agglomeration. These types of agglomerates are rarely observed in TEM and usually exhibit diameters below 1 μm. Thus, the ratio between primary agglomerates and separated MWCNTs can be considered as rather low. Indeed, one major advantage of the three-roll-mill is the low amount of non-dispersed primary agglomerates. In contrast, other dispersion methods, such as stirring or ultrasound, produce MWCNT composites with a higher volume fraction of non-dispersed primary agglomerates which are not impregnated with epoxy resin [52, 53, 56]. Since a steady state of dispersion is reached during processing on the three-roll-mill it is questionable if very small and entangled agglomerates can be separated at all.

Figure 1b depicts the state of dispersion for the binary CB nanocomposites. The CB are well dispersed down to the level of primary particles and small aggregates. These aggregates consist of covalently bonded primary particles. The mean size of the CB aggregates is up to a few hundred nanometres, typical values around 300 nm can be concluded from Fig. 1b. The primary particle size is around 30–40 nm, in good agreement with the manufacturer's data sheet. The breaking-up and dispersion of these structures is unlikely to occur due to mechanical agitation even using a high shear mixing process as done in this work. Comparable to the MWCNT composites, CB composites exhibit a network structure including CB primary particles and CB aggregates.

Already reported in our previous work [14], in ternary nanocomposites based on CB and MWCNTs an intermixing of CB and MWCNTs on the primary particle level can

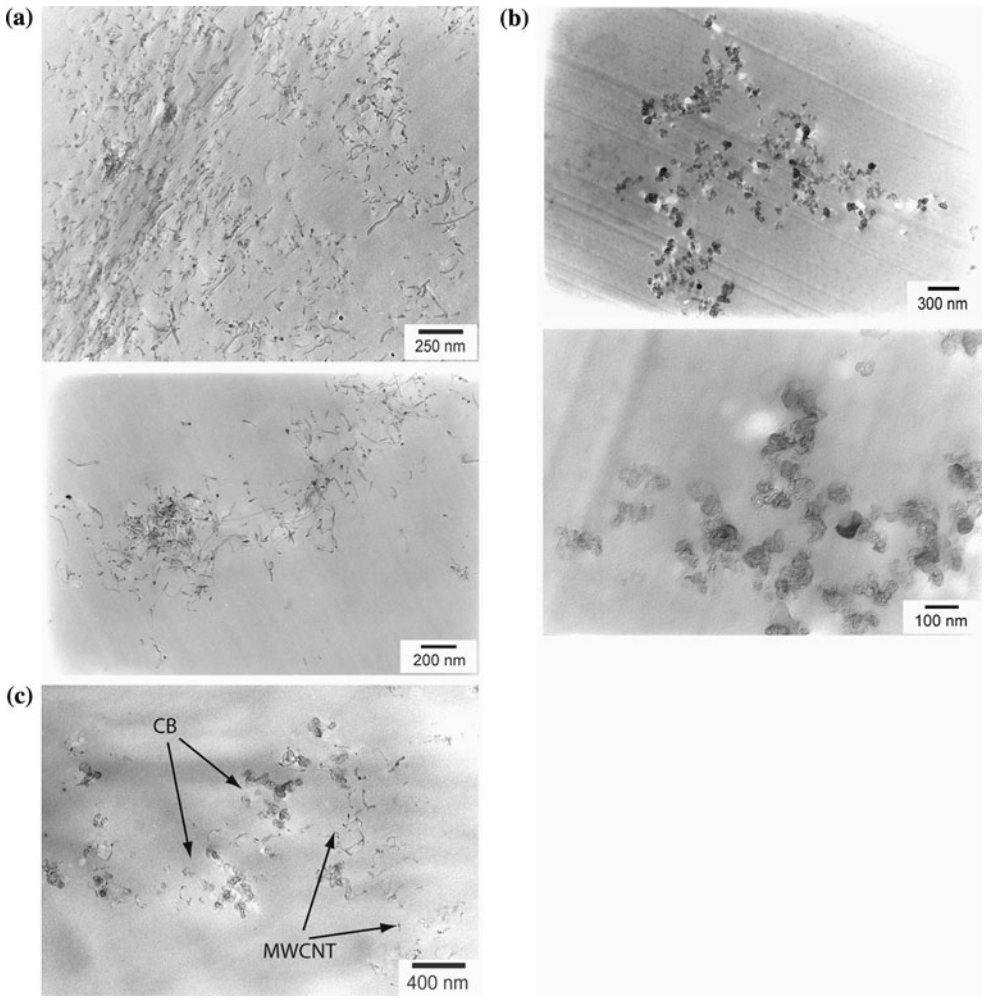


**Fig. 1** TEM-images of a cured nanocomposite with **a** 0.3 wt% of MWCNTs; **b** 0.3 wt% of CB; **c** 0.4 wt% of CB/MWCNTs (0.2 wt% each filler)

be found (see Fig. 1c). As a consequence, co-supporting networks are formed, which were also found for other combinations of carbon based particles [48–50]. In these networks, CB and MWCNTs seem to be randomly distributed. Assuming that different types of carbon nanoparticles (here: CB and MWCNTs) possess similar surface characteristics due to their carbon based atomic structure; it is likely that a good intermixing of both types of particles without a formation of domains or other substructures occurs [57].

## Rheological analysis

Dynamic (oscillatory) measurements yield to the quasi-static rheological data of the nanoparticle filled epoxy suspensions and allow the determination of the elasticity of the nanoparticle network. Beside the evaluation of the binary MWCNT and CB suspensions, the ternary CB/MWCNT suspensions are compared to their binary counterparts. Dynamic rheological experiments deliver various data, such as the storage shear modulus $G'$, the loss shear modulus $G''$ and the loss factor tan $\delta$. In this work, only the storage shear modulus, $G'$, is discussed since it is the most significant parameter for the evaluation of nanoparticle networks in polymers melts or suspensions [33, 38].

Figure 2a shows the $G'$ data as a function of frequency for the binary MWCNT suspensions with filler contents ranging from low (0.03 wt%) to high (1.2 wt%) concentrations. Depending on the MWCNT content, three distinct behaviours can be found. At very low MWCNT contents (0.03 and 0.1 wt%), the frequency spectra do not deviate from the pure epoxy resin system (dashed line). At intermediate MWCNT contents (0.2 and 0.3 wt%), a slight increase in $G'$ at low frequencies can be found, denoting significant changes in the MWCNT network. Nevertheless, the slope of the $G'$–$f$-curve does not differ from the reference curve. At higher MWCNT content (>0.4 wt%), the $G'$–$f$-curve is subsequently shifted to higher $G'$ values.

Additionally, the slope of the $G'$–$f$-curve decreases. With increasing MWCNT content, the slope $G'$–$f$-curve almost levels off, denoting the formation of percolating networks in the suspending epoxy.

Figure 2b depicts the frequency spectra for the binary CB suspensions. Again, the filler content is varied from low (0.03 wt%) to high concentrations (1.6 wt%). As found for the rheological behaviour of the binary MWCNT suspensions, three different behaviours of the $G'$–$f$-curves can be distinguished: first, no change in comparison to the pure epoxy for CB contents up to 0.1 wt%. Second, increases in $G'$ at low $f$ without a change in the slope of the $G'$–$f$-curve for filler contents up to 0.4 wt%. Third, a significant increase in $G'$ together with a lower slope of the $G'$–$f$-curve for CB contents higher than 0.4 wt%. Thus, both general rheological behaviours of the binary MWCNT and CB suspensions appear to be rather similar, reflected by their frequency response. CB particles are subjected to similar agglomeration mechanisms as MWCNTs [58]. Nevertheless, due to the different particle shape of CB and thus different network morphology the CB content at rheological transition as well as the absolute $G'$ values differs from the results found for the binary MWCNT suspensions.

As a third nanoparticle system, ternary CB/MWCNT suspensions were tested (see Fig. 2c). As expected, the general behaviour can be found to be similar to the binary MWCNT and CB suspensions. The absolute values of $G'$ as well as the onset of the rheological transition zone are different from those found for the binary suspensions. As expected, the multi-filler suspensions also exhibit a rheological percolation. The origins of the rheological transition of all tested nanoparticle filled suspensions will be later discussed in detail.

For a deeper discussion of the frequency spectra of the tested suspensions, the curves are fitted by a power law relationship as follows [59, 60]:

$$G'(\omega) = A \cdot f^{\beta} \tag{1}$$

where $\beta$ is the relaxation exponent and $A$ is a constant.

Using Eq. 1, one may obtain Fig. 2d. Here, the relaxation exponent, $\beta$, is plotted against the filler content for both binary MWCNT and CB suspensions as well as the ternary CB/MWCNT suspension. The relaxation exponent, $\beta$, at low filler contents differs significantly from the terminal value for pure Newtonian systems ($\beta = 2$). In literature, lower values than 2 are reported for polymer melts with a broad molecular weight distribution [61]. However, in the uncured epoxy monomer system, a relaxation exponent of roughly 0.6–0.8 is found. Since the measurements are performed within the linear visco-elastic regime, one reason may be found in the resolution limit of the force transducer. The pure epoxy system LY556/CH917 exhibit an apparent viscosity of roughly 0.6 which leads to very low $G'$ at low frequencies ($\sim 10^{-1}$ Pa). Thus, the relaxation exponent for such low structured systems may be overestimated by the fitting. Nevertheless, for low filled suspensions the exponent scatters in the regime mentioned above. Above a critical filler content, the relaxation exponent starts to decrease. The onset of the decrease is somewhat dependent on the type of nanoparticle used. The relaxation exponent of the binary MWCNT suspensions decreases asymptotically at the lowest filler contents. In comparison, the relaxation exponent for the CB systems decreases at the highest filler contents. The ternary CB/MWCNT mixture is situated between both binary systems. The decrease of the relaxation exponent is related to an entanglement transition where the nanoparticles form an interconnected network in the suspension [27, 60]. At high filler loadings, all systems exhibit a decreased low-frequency power-law scaling at a level of 0.1, reflecting an almost frequency independent storage modulus $G'$ and thus solid-like rheological behaviour. Interestingly, the decrease of the relaxation exponent of the binary CB suspension takes place in a broader filler content regime as the decrease of the binary MWCNT suspensions. This may be explained in terms of the less robust CB network formed once the critical filler content for mechanical interlocking of nanoparticles is reached.

As mentioned earlier, nanoparticle filled suspensions undergo a rheological transition once a critical filler content for the formation of an entangled and mechanical rigid network is reached. These agglomerate networks are reflected by the elastic storage modulus $G'$ in the terminal region. Thus, the $G'$ data at 0.5 Hz are plotted against the filler content for the MWCNT, CB and CB/MWCNT suspensions, leading to a rheological percolation diagram (see Fig. 2e).

The binary MWCNT suspensions show an increase in storage modulus $G'$ at the lowest filler content in comparison to the other tested suspensions. The binary CB suspensions exhibit a significant increase in $G'$ at the highest filler contents. The ternary CB/MWCNT suspensions are situated between both binary systems. In order to perform a deeper analysis on the rheological percolation, the data of the three systems are fitted by the statistical percolation theory [62, 63] in analogy to the fitting performed for the electrical conductivity of the cured systems in our previous work [14]:

$$G = G_0\left(\Phi - \Phi_{\mathrm{c,rheo}}\right)^{t_{\mathrm{rheo}}} \tag{2}$$

where $\Phi$ is the filler content and $\Phi_{\mathrm{c,rheo}}$ the percolation threshold, $G_0$ storage shear modulus at $\Phi_{\mathrm{c,rheo}}$ and $t_{\mathrm{rheo}}$ the percolation exponent. According to [63], the percolation threshold in the fitting was incrementally changed ($\Delta\Phi = 0.01$ wt%) in order to obtain a best fit of the rheological data. Figure 2f and Table 1 show the results of the fitting in detail.

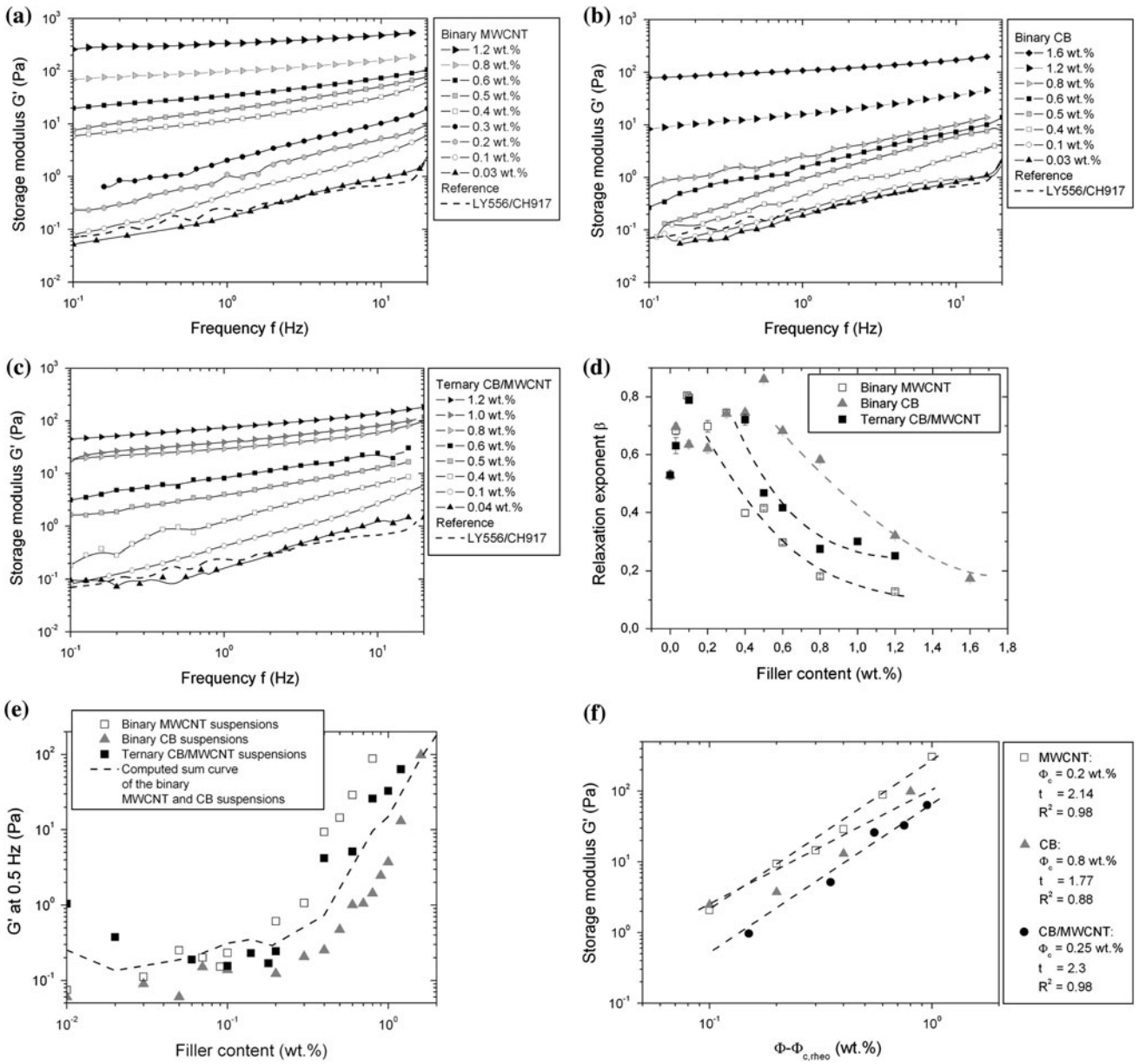


**Fig. 2** $G'$ versus $f$ for suspensions with varying **a** MWCNT content; **b** CB content; **c** CB/MWCNT content at fixed CB:MWCNT ratio. **d** Relaxation exponent $\beta$ versus filler content for the tested suspensions.**e** Storage modulus$G'$ for the MWCNT, CB and CB/MWCNT suspensions exhibiting percolation behaviour. **f** Fitted curves according to the percolation law for the MWCNT, CB and CB/MWCNT suspensions

The binary MWCNT suspensions exhibit the lowest rheological percolation threshold of all tested systems at a critical filler content of 0.2 wt%. The CB suspensions possess a higher threshold of 0.8 wt%. The difference of both rheological percolation thresholds is usually explained by the high aspect ratio of the MWCNTs forming an agglomerate network at subsequently lower filler contents. Considering the extended model of the percolation theory based on cluster aggregation mechanisms for the development of a network structure as proposed by Alig et al. [20, 21, 40, 47] and used by Deng et al. [58], it seems likely that the agglomerate size is a crucial parameter for the rheological percolation threshold. Here, fibre-like particles such as MWCNTs tend to form greater and mechanically

**Table 1** Rheological data of the binary and ternary suspensions derived from Fig. 2f

| Suspension | $\Phi_{c,rheo}$ (wt%) | $t_{rheo}$ | $G'$ at 0.8 wt% (Pa) |
|---|---|---|---|
| Binary MWCNT | 0.2 | 2.1 | 88.4 |
| Binary CB | 0.8 | 1.8 | 1.4 |
| Ternary CB/MWCNT | 0.25 | 2.3 | 25.9 |

more rigid agglomerates as CB. The ternary CB/MWCNT suspensions exhibit a threshold of 0.25 wt%, which is almost identical to the threshold of the binary MWCNT suspensions.

All tested suspensions (MWCNT, CB and CB/MWCNT) exhibit similar rheological percolation exponents between 1.8 and 2.3. From theory, a rheological percolation exponent of $2.1 \pm 0.2$ belong to percolating bonds, which resist stretching but are free to rotate [64]. This theoretical value correlates rather well with the experimental results of the tested suspensions (see Table 1) as well as of other types of CNT suspensions [30]. Although there might be other possible mechanisms such as bending of particles [65], the high stiffness of MWCNTs and CB aggregates leads to the conclusion that the CB and MWCNT networks are composed of freely connected particles. The slight difference of the rheological percolation exponents of the binary MWCNT and binary CB suspensions may be explained in terms of higher network strength of the MWCNT network above percolation. In addition to freely joined bonds, the long aspect ratio of the MWCNTs leads to entanglements and thus mechanical interlocking in suspended media. It has to be mentioned that a much higher rheological percolation exponent ($\sim 4.2$) was found for a similar system as used in this work (MWCNT Graphistrength C100® and LY556) [45]. Since the percolation theory has its limitations in describing agglomeration phenomena of CNTs and CB it has to be emphasised that the discussion of the fit parameters (e.g. percolation exponent) can only lead to a basic picture of the actual agglomerate structure and needs to be studied in-depth, based on other mechanical mixing laws, e.g. as performed in [20, 21, 40, 47].

The percolation threshold of multi-filler (ternary) systems cannot be derived from a simple addition of the thresholds of the respective binary systems. Thus, the model from Sun et al. [50] is used to compare experimental and theoretical results, which was already performed in our previous work for the electrical percolation threshold of the cured systems [14]. According to [50], the percolation threshold of ternary systems can be estimated by adopting the 'excluded volume' approach from Balberg [66]:

$$\frac{m_{\mathrm{CB}}}{\Phi_{\mathrm{CB,binary}}} + \frac{m_{\mathrm{MWCNT}}}{\Phi_{\mathrm{MWCNT,binary}}} = 1 \tag{3}$$

where $m_{\mathrm{CB}}$ and the $m_{\mathrm{MWCNT}}$ are the mass fractions in the ternary systems, $\Phi_{\mathrm{CB,binary}}$ and $\Phi_{\mathrm{CNT,binary}}$ the respective percolation thresholds in the binary systems. Using the experimental results of the percolation thresholds and rearranging Eq. 3 one may have

$$0.8 \cdot m_{\mathrm{CB}} + 0.2 \cdot m_{\mathrm{MWCNT}} = 0.16\,\mathrm{wt\%} \tag{4}$$

In this work, $m_{\mathrm{CB}}$ equals $m_{\mathrm{MWCNT}}$ since the relative ratio of CB and MWCNT is set to 50:50%. Using Eq. 4 one may obtain for the rheological percolation threshold of the ternary CB/MWCNT system:

$$\Phi_{\mathrm{ternary,rheo}} = 2 \cdot m_{\mathrm{CB}} = 2 \cdot m_{\mathrm{MWCNT}} = 0.32\,\mathrm{wt\%} \tag{5}$$

The rather small difference of the computed and experimental rheological percolation threshold of the ternary CB/MWCNT does not lead to a concluding remark about synergistic effects of nanoparticle intermixing on the rheological percolation threshold. The small difference in theoretical and experimental threshold was also found for the electrical conductivity of the cured ternary systems [14]. Nevertheless, if synergistic effects occur in ternary systems in terms of their network morphology, it seems likely that these networks are already present in the suspension directly after dispersion on the three-roll-mill. Nevertheless, the difference in $G'$ at higher filler contents between the computed sum curve in Fig. 2e and the experimental results for ternary CB/MWCNT suspensions are higher than the difference of the electrical conductivities in the cured state (compare Figs. 4.5 and 1 in [14]). This may be due to a change in morphology of the co-supporting networks during curing. Indeed, a partial alignment of MWCNTs during dynamic re-agglomeration may promote the dominating effect of MWCNT in cured ternary CB/MWCNT systems which are not that pronounced in the uncured state [67].

## Comparison of rheological and electrical percolation

As mentioned earlier, in nanoparticle filled epoxy the particle network morphology is strongly dependent on kinetic agglomeration mechanisms in the uncured state prior or during curing. A comparison of the rheological and electrical percolation transition can give a comprehensive insight in the network forming processes and is further discussed among the various tested systems (MWCNTs, CB and CB/MWCNTs). Thus, the different percolation phenomena found in electrical conductivity of the cured nanocomposites as well as in rheological properties of the nanoparticle filled suspensions is discussed. Additionally, the electrical conductivity of the uncured suspensions was measured during rheological measurements.

Figure 3a shows the electrical conductivity of the cured binary MWCNT systems together with the storage shear modulus, $G'$, and the electrical conductivity of the respective suspensions. The percolation region of the electrical conductivity of the cured nanocomposites occurs at lower MWCNT contents as the percolation region for $G'$ and the electrical conductivity of the uncured suspensions. The difference of the percolation thresholds is roughly one order of magnitude (0.025 vs. 0.2 wt%) (see also Table 2). This significant reduction of percolation onset can be

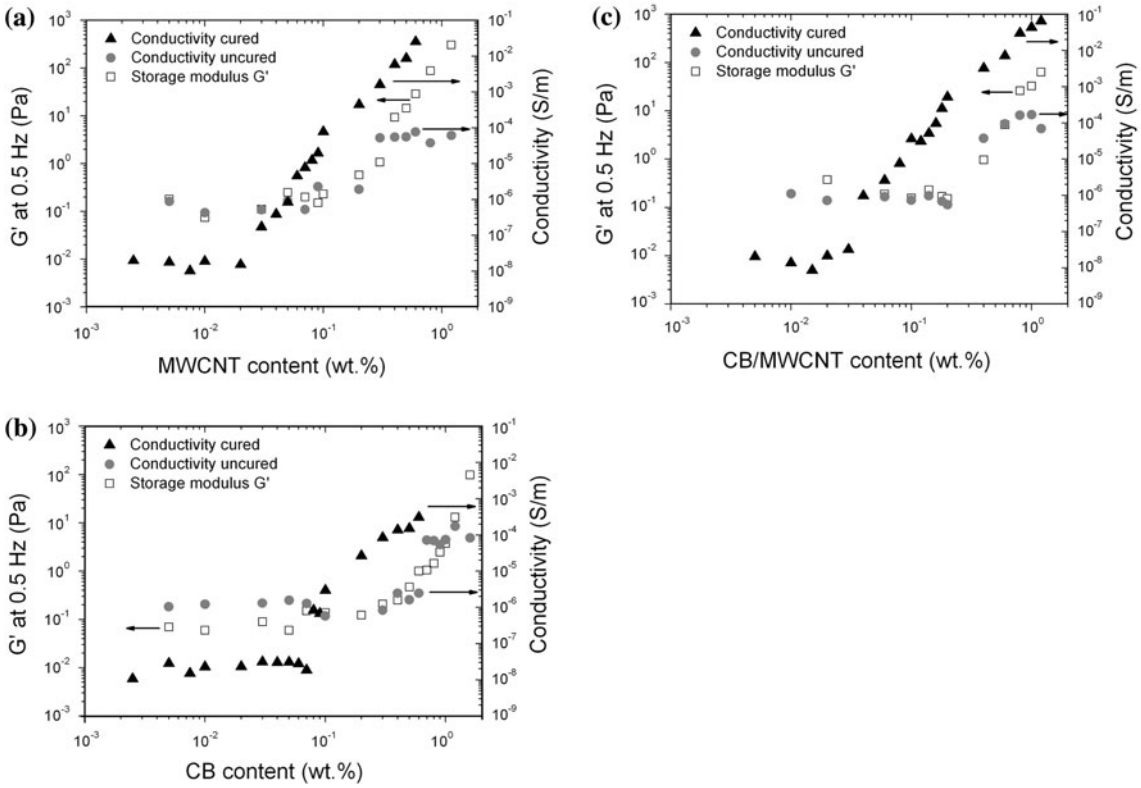


**Fig. 3** Comparison of electrical conductivity of the cured nanocomposites with the storage shear modulus, $G'$, and electrical conductivity of the suspensions for the **a** binary MWCNT systems; **b** binary CB systems; **c** ternary CB/MWCNT systems. Electrical conductivity data of the cured systems is taken from [14]

**Table 2** Rheological and electrical percolation data of the binary and ternary suspensions

| Nanocomposite | $\Phi_{c,el,cured}$ (wt%) | $\Phi^{a}_{c\ el,uncured}$ (wt%) | $\Phi_{c,rheo}$ (wt%) |
|---|---|---|---|
| Binary MWCNT | 0.025 | ~0.2 | 0.2 |
| Binary CB | 0.085 | ~0.8 | 0.8 |
| Ternary CB/MWCNT | 0.03 | ~0.25 | 0.25 |

[a] Not determined by fitting, simple estimation from Fig. 3a to c

attributed to the dynamic re-agglomeration processes occurring during curing which is usually promoted by the introduction of shear forces due to mechanical agitation or temperature gradients in the mould. In case of the used anhydride cured epoxy system, re-agglomeration is further promoted by the low viscosity of the resin system (~0.6 Pas) as well as its relatively high acidity leading to low surfaces charges of the nanoparticles [6, 68]. Since the epoxy systems do not consist of large molecule chains this decrease in percolation threshold during curing may hold for every CNT thermoset system although it may vary in its magnitude. In contrast, thermoplastic systems usually exhibit higher electrical percolation thresholds than their rheological ones due to the formation of a combined polymer-CNT network which increases the rheological properties without establishing a conductive network [37–39, 69]. Additionally, thermoplastic systems do not exhibit such strong dynamic re-agglomeration during vitrification due to their high viscosity in the molten state.

Regarding the electrical conductivity of the uncured binary MWCNT suspensions, it can be seen that the electrical and rheological transitions take place at the same MWCNT content (~0.2 wt%), emphasising the assumption of negligible particle–epoxy monomer interactions. In other words, if no interactions between particles and epoxy molecules exist, an increase in rheological properties is only due to the formation of a particle network. In turn, the electrical conductivity increases if the rheological properties increase. Furthermore, the rheological percolation threshold can be considered as an upper boundary for the electrical percolation threshold, also for cured systems. It seems unlikely that the electrical percolation threshold can become higher than the rheological one.

Two special phenomena of the electrical conductivity of the uncured MWCNT suspensions must be addressed. First, the electrical conductivity at low filler contents in the uncured state is higher as found in the cured state. This high

level is mainly caused by the ion conductivity of the LY556/CH917 mixture. The ion conductivity of the neat resin system decreases with increasing degree of conversion during curing. On the other hand, the dynamic re-agglomeration of MWCNTs is promoted by an increase in temperature. The formed networks lead to an increase in conductivity. Thus, a maximum in conductivity is obtained near the gel point where both, the particle network and the epoxy matrix, are conductive [70]. Afterwards, the conductivity decreases to the level of the cured nanocomposite.

Second, at high filler contents, the electrical conductivity levels off at roughly $10^{-4}$ S/m while the storage shear modulus, $G'$, still increases with increasing filler content. The origin of such behaviour can be manifold. The difference in electrical conductivity in the cured and uncured state at high filler contents is up to three orders of magnitude. Since both states provide dense networks, it seems likely that the mean interparticle separation for electron tunnelling must be higher in the uncured state. The mechanism of charge carrier tunnelling is regarded to be the determining network parameter in polymers filled with conductive particles [71, 72]. A higher interparticle separation is probably due to Brownian motions acting on the MWCNTs as well as a different relative permittivity of the suspensions in comparison to the cured epoxy. Another reason may be the experimental setup of the rheometer. A resin-rich exclusion layer may be formed between the plates of the rheometer leading to constant conductivities at higher filler contents. Furthermore, agglomerate structures may be formed which shortcuts the small gap size of 500 μm between the electrodes. At higher filler contents, the number and size of flocs or agglomerates increase but their impact on the electrical conductivity may be weak since conductive pathways between the rheometer plates already exist. On the other hand, increasing filler content may lead to higher $G'$ since a more homogeneous network is created. In general, it seems likely, that a particle network for electrical conductivity can be rather inhomogeneous while a network for rheological properties should exhibit a more homogeneous particle or agglomerate distribution.

Figure 3b, c depict the comparison of electrical and rheological data of the binary CB and ternary CB/MWCNT systems. Interestingly, as found for the binary MWCNT systems, the difference between the onset of percolation in the cured state and in the uncured state ranges also in one order of magnitude (see also Table 2). Additionally, the electrical and rheological percolation thresholds of the suspensions coincidence for both binary CB and ternary CB/MWCNT systems. As found for the binary MWCNT suspensions, the electrical conductivity levels off at $10^{-4}$ S/m for high filler contents. Since the main features of the percolation curves are similar for all tested nanoparticle systems (MWCNT, CB and CB/MWCNT) it seems likely that the acting mechanisms for network formation during curing are rather independent on the particle morphology. Deng et al. [58] suggested similar agglomeration mechanisms for CNT and CB systems based on a cluster aggregation model proposed by Alig et al. [20, 21, 40, 47]. The results derived from percolation studies in this work support these assumptions. The size of clusters (or agglomerates) may determine the relative position of the percolation thresholds of the various systems though the constant difference of electrical and rheological percolation thresholds strongly support the suggestions of similar aggregation mechanisms of CNT and CB filled epoxy systems [58]. Together with their entangled structure the length of the MWCNTs used in this work is at roughly 1 μm [73]. Thus, such types of industrially available CVD-MWCNTs may not have special features of long aspect ratio CNTs (e.g. in aligned CNT carpets).

The difference of electrical conductivity of the binary CB systems in the uncured and cured state is much lower than the differences found for the binary MWCNT systems. A lower tendency for re-agglomeration during curing could cause this effect. Nevertheless, the constant difference of rheological and electrical percolation threshold of both binary systems (CB and MWCNT) of one order of magnitude does not support such assumptions. It seems more likely that the mean interparticle separation of CB aggregates does not change during curing while it changes in the binary MWCNT suspensions. In that sense, the MWCNTs in the ternary CB/MWCNT systems seem to govern the charge carrier transport mechanisms since an increase in electrical conductivity during curing was found similar to the increase in electrical conductivity of the binary MWCNT systems. This dominating role was already proposed in our previous work and meanwhile theoretically proven by Rahatekar et al. [67].

Lott [74] found a difference of one order of magnitude between electrical percolation thresholds in the cured and uncured state for another CNT epoxy system (amine hardened). Thus, it can be concluded that the aggregation mechanisms acting on the nanoparticles are also independent on the chemical nature of the epoxy system if the particle are randomly distributed. Only the viscosity level at curing temperature and the resulting convection shear forces acting on the suspensions govern the cluster aggregation or flocculation mechanisms.

## Conclusions

In this work, quasi-static rheological experiments with in situ conductivity measurements were conducted for MWCNT, CB and CB/MWCNT filled epoxy suspensions.

Independent on the type of filler, increasing filler content leads to a change in the frequency response including a non-terminal behaviour reflecting a solid-like behaviour of suspensions with high filler contents.

The rheological percolation threshold of the binary MWCNT suspensions is the lowest of all tested systems (0.2 wt%). The binary CB systems exhibit a four-times higher rheological percolation threshold of 0.8 wt% which can be explained by the spherical shape of the CB particles in contrast to the fibrous MWCNTs. Thus, a network throughout the suspensions is created at subsequently lower filler contents in the binary MWCNT suspensions. The ternary CB/MWCNT systems exhibit a rheological percolation threshold of 0.25 wt%. Theoretical predictions about the percolation threshold using the excluded volume approach cannot give a consistent statement about synergistic effects in network morphology in multi-filler systems although results in $G'$ above percolation threshold may support these assumptions. Nevertheless, it could be shown, that co-supporting networks are already present in the suspension directly after dispersion and were not formed during curing. It can be stated that the impact of co-supporting networks in multi-filler systems is more pronounced in the cured state as in the uncured state.

The electrical percolation threshold in the uncured state and the rheological percolation threshold coincidence, emphasising that nanoparticle–epoxy interactions are unlikely to occur in uncured suspensions. The electrical percolation threshold in the cured state is always lower than the rheological one due to re-agglomeration processes during curing. Regarding the three different nanoparticle systems (MWCNT, CB and CB/MWCNT) the difference between both percolation thresholds is constant, roughly one order of magnitude. This is due to similar re-agglomeration mechanisms such as cluster aggregation acting on the nanoparticles rather independently on their geometrical shape (spherical or fibrous). Thus, the overall lower percolation thresholds (rheological and electrical) of MWCNT systems in comparison to CB systems may not arise from a higher tendency for network formation of MWCNTs. Their fibre-like shape may lead to greater agglomerates and thus lower interparticle separation and less number of tunnelling resistances.

Since industrially available MWCNTs are rather short, they generally behave very similar to CB with shifted properties such as the electrical conductivity and elasticity (viscosity) and related parameters. It is known that these properties are sensitive to shear applied to suspensions. Ongoing research of our group will show the shear-dependent properties of such networks in terms of rheology and electrical conductivity.

**Acknowledgements** The German Research Foundation (Deutsche Forschungsgemeinschaft) and its graduate school 'Kunst und Technik' at the Technische Universität Hamburg-Harburg is gratefully acknowledged for financial support (DFG GRK 1006/1). The companies Degussa-Evonik® and Arkema® are acknowledged for supplying the nanoparticles.

## References

1. Thostenson ET, Li CY, Chou TW (2005) Compos Sci Technol 65:491
2. Chung DDL (2004) J Mater Sci 39:2645. doi:10.1023/B:JMSC0000021439.1802.ea
3. Winey KI, Kashiwagi T, Mu M (2007) MRS Bull 32:348
4. Ezquerra TA, Kulescza M, Baltá-Calleja FJ (1991) Synth Met 41:915
5. Prasse T, Flandin L, Schulte K, Bauhofer W (1998) Appl Phys Lett 72:2903
6. Flandin L, Prasse T, Schueler R, Schulte K, Bauhofer W, Cavaille J (1999) Phys Rev B 59:14349
7. Ezquerra TA, Connor MT, Roy S, Kulescza M, Fernandes-Nascimento J, Baltá-Calleja FJ (2001) Compos Sci Technol 61:903
8. Thostenson ET, Ren ZF, Chou TW (2001) Compos Sci Technol 61:1899
9. Moniruzzaman M, Winey KI (2006) Macromolecules 39:5194
10. Coleman JN, Khan U, Gun'ko YK (2006) Adv Mater 18:689
11. Baughman RH, Zakhidov AA, de Heer WA (2002) Science 297:787
12. Chou T, Gao L, Thostenson ET, Zhang Z, Byun J (2010) Compos Sci Technol 70:1
13. Gojny FH, Wichmann MH, Fiedler B, Kinloch IA, Bauhofer W, Windle AH, Schulte K (2006) Polymer 47:2036
14. Sumfleth J, Adroher XC, Schulte K (2009) J Mater Sci 44:3241. doi:10.1007/s10853-009-3434-7
15. Sandler J, Shaffer MSP, Prasse T, Bauhofer W, Schulte K, Windle AH (1999) Polymer 40:5967
16. Bryning MB, Islam MF, Kikkawa JM, Yodh AG (2005) Adv Mater 17:1186
17. Bauhofer W, Kovacs JZ (2009) Compos Sci Technol 69:1486
18. Martin CA, Sandler JKW, Shaffer MSP, Schwarz MK, Bauhofer W, Schulte K, Windle AH (2004) Compos Sci Technol 64:2309
19. Kharchenko SB, Douglas JF, Obrzut J, Grulke EA, Migler KB (2004) Nat Mater 3:564
20. Alig I, Skipa T, Engel M, Lellinger D, Pegel S, Pötschke P (2007) Phys Status Solidi B 244:4223
21. Alig I, Lellinger D, Engel M, Skipa T, Pötschke P (2008) Polymer 49:1902
22. Skipa T, Lellinger D, Böhm W, Saphiannikova M, Alig I (2010) Polymer 51:201
23. Richter S, Grenzer M, Jehnichen D, Bierdel M, Heinrich G (2009) Express Polym Lett 3:753
24. Fan Z, Advani SG (2007) J Rheol 51:585
25. Rahatekar SS, Koziol KKK, Butler SA, Elliott JA, Shaffer MSP, Mackley MR, Windle AH (2006) J Rheol 50:599
26. Shaffer MSP, Fan X, Windle AH (1998) Carbon 36:1603
27. Shaffer MSP, Windle AH (1999) Macromolecules 32:6864
28. Kinloch IA, Roberts SA, Windle AH (2002) Polymer 43:7483
29. Xu JH, Chatterjee S, Koelling KW, Wang YR, Bechtel SE (2005) Rheol Acta 44:537
30. Hough LA, Islam MF, Janmey PA, Yodh AG (2004) Phys Rev Lett 93:1
31. Hobbie EK, Fry DJ (2007) J Chem Phys 126:1
32. Huang YY, Ahir SV, Terentjev EM (2006) Phys Rev B 73:125422
33. Pötschke P, Fornes TD, Paul DR (2002) Polymer 43:3247
34. Abbasi S, Carreau PJ, Derdouri A (2010) Polymer 51:922

35. Zhang Q, Rastogi S, Chen D, Lippits D, Lemstra PJ (2006) Carbon 44:778
36. Bangarusampath DS, Ruckdäschel H, Altstädt V, Sandler JKW, Garray D, Shaffer MSP (2009) Chem Phys Lett 482:105
37. Du FM, Scogna RC, Zhou W, Brand S, Fischer JE, Winey KI (2004) Macromolecules 37:9048
38. Pötschke P, Abdel-Goad M, Alig I, Dudkin S, Lellinger D (2004) Polymer 45:8863
39. Hu GJ, Zhao CG, Zhang SM, Yang MS, Wang ZG (2006) Polymer 47:480
40. Alig I, Skipa T, Lellinger D, Pötschke P (2008) Polymer 49:3524
41. Kotsilkova R, Fragiadakis D, Pissis P (2005) J Polym Sci B 43:522
42. Song YS, Youn JR (2005) Carbon 43:1378
43. Moisala A, Li Q, Kinloch IA, Windle AH (2006) Compos Sci Technol 66:1285
44. Battisti A, Skordos AA, Partridge IK (2009) Compos Sci Technol 69:1516
45. Allaoui A, El Bounia N (2010) Curr Nanosci 6:158
46. Chapartegui M, Markaide N, Florez S, Elizetxea C, Fernandez M, Santamaria A (2010) Compos Sci Technol 70:879
47. Alig I, Lellinger D, Dudkin SM, Pötschke P (2007) Polymer 48:1020
48. Li J, Wong P, Kim JK (2008) Mater Sci Eng A 483:660
49. Bokobza L, Rahmani M, Belin C, Bruneel JL, El Bounia N (2008) J Polym Sci B 46:1939
50. Sun Y, Bao H, Guo Z, Yu J (2009) Macromolecules 42:459
51. Ma P, Liu M, Zhang H, Wang S, Wang R, Wang K, Wong Y, Tang B, Hong S, Paik K, Kim J (2009) ACS Appl Mater Interfaces 1:1090
52. Gojny FH, Wichmann MHG, Kopke U, Fiedler B, Schulte K (2004) Compos Sci Technol 64:2363
53. Gojny FH, Wichmann MHG, Fiedler B, Schulte K (2005) Compos Sci Technol 65:2300
54. Wichmann MHG, Sumfleth J, Fiedler B, Gojny FH, Schulte K (2006) Mech Compos Mater 42:395
55. Kovacs JZ, Velagala BS, Schulte K, Bauhofer W (2007) Compos Sci Technol 67:922
56. Gojny FH, Wichmann MHG, Fiedler B, Bauhofer W, Schulte K (2005) Composites A 36:1525
57. Zhang W, Blackburn RS, Dehghani-Sanij AA (2007) Scripta Mater 56:581
58. Deng H, Skipa T, Zhang R, Lellinger D, Bilotti E, Alig I, Peijs T (2009) Polymer 50:3747
59. Wang M, Wang W, Liu T, Zhang W (2008) Compos Sci Technol 68:2498
60. Abraham TN, Ratna D, Siengchin S, Karger-Kocsis J (2008) J Appl Polym Sci 110:2094
61. Krishnamoorti R, Giannelis EP (1997) Macromolecules 30:4097
62. Stauffer D, Aharony A (1992) Introduction to percolation theory. Taylor & Francis, London
63. Kilbride BE, Coleman JN, Fraysse J, Fournet P, Cadek M, Drury A, Hutzler S, Roth S, Blau WJ (2002) J Appl Phys 92:4024
64. Sahimi M, Arbabi S (1993) Phys Rev B 47:703
65. Head DA, MacKintosh FC, Levine AJ (2003) Phys Rev E 68:25101
66. Balberg I, Anderson CH, Alexander S, Wagner N (1984) Phys Rev B 30:3933
67. Rahatekar SS, Shaffer MSP, Elliott JA (2010) Compos Sci Technol 70:356
68. Prasse T, Schwarz MK, Schulte K, Bauhofer W (2001) Colloid Surf A 189:183
69. Zhang QH, Lippits DR, Rastogi S (2006) Macromolecules 39:658
70. Schwarz M (2006) Cuvillier, Dissertation, TU Hamburg-Harburg
71. Sheng P, Sichel EK, Gittleman JI (1978) Phys Rev Lett 40:1197
72. Li C, Thostenson ET, Chou TW (2007) Appl Phys Lett 91:223114
73. Rosca ID, Hoa SV (2009) Carbon 47:1958
74. Lott J (2009) Dissertation, TU Hamburg-Harburg